CHEMISTRY
A EUROPEAN JOURNAL

Design and Self-Assembly of Ditopic and Tetratopic Cavitand Complexes

Edoardo Menozzi,[a] Marco Busi,[a] Romina Ramingo,[a] Mara Campagnolo,[b] Silvano Geremia,[b] and Enrico Dalcanale*[a]

Abstract: The self-assembly of open ditopic and tetratopic cavitand complexes has been investigated by using monofunctionalized cavitand ligands and suitable metal precursors. In the case of ditopic complexes, self-assembly protocols, leading exclusively to the formation of both thermodynamically stable *cis*-Pt square-planar complexes **8** and **9** and the kinetically inert *fac*-Re octahedral complex **14**, have been elaborated. The use of *cis*-[Pt$(CH_3CN)_2Cl_2$] as metal precursor led to the formation of monotopic *trans*-**10** and ditopic *trans*-**11** cavitand complexes, while *cis*-[Pt$(dmso)_2Cl_2$] afforded both *cis*-**13** and *trans*-**11** isomers. The self-assembly of tetratopic cavitand complexes has been achieved by using mononuclear [Pd$(CH_3CN)_4$-$(BF_4)_2$] and dinuclear [M_2(tppb)$(OTf)_4$] (**19**: M = Pt; **20**: M = Pd) metal precursors. Only the tetratopic dinuclear complexes **21** and **22** were stable. The ligand configuration with two phosphorus and two cavitand ligands at the metal centers is the most appropriate to build tetratopic cavitand complexes with sufficient kinetic stability.

Keywords: cavitands · metal–ligand interactions · self-assembly · supramolecular chemistry

Introduction

This work reports a detailed study of the self-assembly of open ditopic and tetratopic cavitand complexes, with the aim of providing reliable synthetic protocols for the formation of multitopic molecular receptors.

While the design and formation of self-assembled molecular containers, such as calixarene-based capsules[1] and cavitand-based coordination cages,[2] have received much attention, the corresponding self-assembly of open multitopic receptors has been neglected so far. One reason is related to the need for partially derivatized precursors, which are synthetically more demanding than the corresponding fully derivatized ones. Thus far, research activity has been focused on the formation of covalently linked ditopic calixarene[3] and cavitand[4] receptors, with the purposes of enlarging the cavity space and achieving cooperativity in the bonding of complementary guests. The typical approach requires two calixarene or cavitand receptors connected in a face-to-face manner through a linker molecule. In the case of a single linker molecule, flexible structures are obtained, while insertion of a second linker molecule leads to conformationally fixed, clamshell-type structures (Figure 1).

Our approach to the self-assembly of multitopic cavitand complexes is based on metal–ligand interactions. The major advantages of using transition metals for self-assembly are: 1) the great directionality offered by metal–ligand coordinative bonds relative to weak electrostatic and π–π-stacking interactions or even hydrogen bonding; and 2) the possibility of fine-tuning the kinetic stability of coordinative bonds by the appropriate choice of metal precursors and ligands.[5] The final shape of the self-assembled entity is not only defined by the coordination geometry of the metal-complex, but also by the orientation of the ligand interaction sites. The most common building blocks are decorated with nitrogen- and phosphorus-based ligands. Within this context, the following steps have been devised for the preparation of ditopic and tetratopic cavitand receptors: 1) the synthesis of monofunctionalized cavitands bearing a pyridine ligand at the upper rim, and 2) the exploration of the coordination chemistry of these cavitand ligands to find synthetic protocols leading to the formation of both thermodynamically

[a] Dr. E. Menozzi, Dr. M. Busi, Dr. R. Ramingo, Prof. E. Dalcanale
Dipartimento di Chimica Organica ed Industriale and Unità INSTM
Università degli Studi di Parma
Parco Area delle Scienze 17/A, 43100 Parma (Italy)
Fax: (+39) 0521-905-472
E-mail: enrico.dalcanale@unipr.it

[b] Dr. M. Campagnolo, Prof. S. Geremia
Dipartimento di Scienze Chimiche, Università di Trieste
Via L. Giorgeri 1, 34127 Trieste (Italy)

Supporting information for this article is available on the WWW under http://www.chemeurj.org/ or from the author.

DOI: 10.1002/chem.200401061

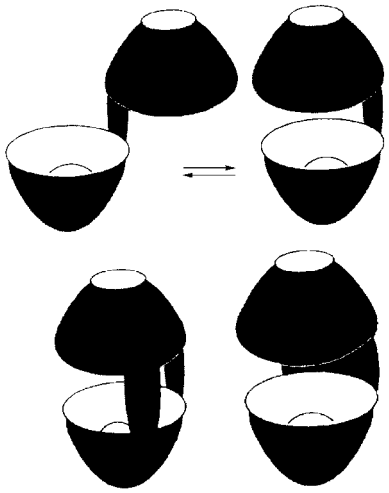

Figure 1. Cartoon representation of covalently linked ditopic receptors. Above: flexible structures obtained by using a single linker molecule. Below: conformationally fixed, clamshell-type structures resulting from the insertion of a second linker molecule.

and kinetically stable complexes presenting concave surfaces of molecular dimensions.

Results and Discussion

Synthesis of monofunctionalized cavitand ligands: Four related cavitand ligands of general structure **A** and **B** were designed and prepared. They have in common three methylene bridges, which do not interfere with metal–ligand coordination. The fourth bridge has a pyridyl substituent in the case of **A** and a larger 4-phenylpyridyl one in **B**, both in the desired outward configuration. Two different alkyl chain substituents, positioned at the lower rim, were chosen to improve the solubility of the ligands in apolar solvents (R: $C_{11}H_{23}$) or to favor the formation of single crystals for X-ray structure determination (R: C_2H_5).

The three methylene bridges were introduced in the resorcinarene building blocks by using dibromomethane as bridging reagent in a 2.2:1 molar ratio with respect to the resorcinarene. Working with a stoichiometric defect of CH_2Br_2 for short reaction times reduced the amount of undesired tetramethylene-bridged cavitand. The final bridging reaction was performed by adding an excess of 4-(α,α′-dibromomethyl)pyridine or 4-(α,α′-dibromotolyl)pyridine to a solution of partially bridged resorcinarenes **1** and **2** in DMA in the presence of K_2CO_3 as base (Scheme 1).

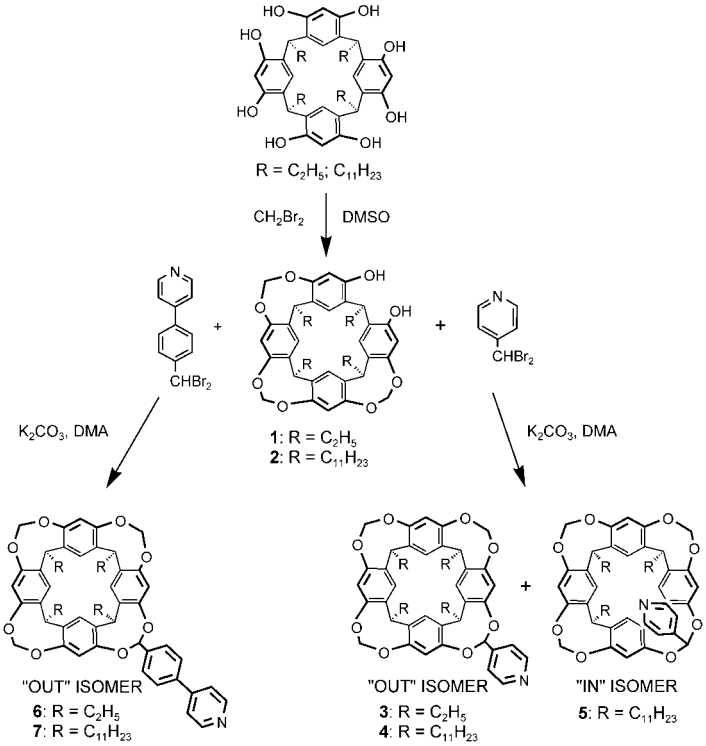

Scheme 1. Synthesis of monofunctionalized cavitand ligands **3**–**7**.

The stereochemical outcome of the two reactions was different: the reaction with 4-(α,α′-dibromomethyl)pyridine led to the formation of both "out" (i.e., outward configuration) and "in" (i.e., inward configuration) isomers, **4** and **5**, respectively, in a 1:2 ratio (in the case of **3**, the corresponding "in" isomer was not purified). This behavior was in contrast to the complete stereoselectivity toward the "out" isomer observed in the case of the bridging reaction with benzal bromide.[6] More recently, the absence of stereochemical control has also been reported with a related pyridyl bridging group.[7] However, here, complete stereoselectivity toward the "out" isomer was obtained by using 4-(α,α′-dibromotolyl)pyridine as a bridging reagent, which cannot be easily accommodated within the cavity in the inward configuration (cavitands **6** and **7**).

The self-assembly driven by metal coordination required cavitands with the pyridine ligands in a diverging spatial orientation with respect to the cavity. Therefore, only the "out" isomers were useful for the purpose.

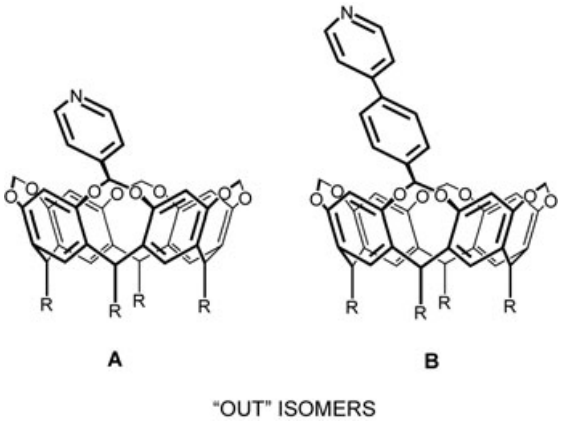

Self-assembly of ditopic complexes: Metal-connected ditopic cavitands were obtained by following the typical cage self-assembly protocol.[8] The exclusive formation of the desired *cis* ditopic complex was assured by the presence of the bidentate dppp ligand, which left only the *cis* positions accessible to ligand exchange. The procedure for self-assembly of ditopic complexes is shown in Scheme 2: by mixing the cavitand (either **4** or **6**) with $[Pt(dppp)(CF_3SO_3)_2]$ (2:1 molar ratio) at room temperature in solvents such as $CHCl_3$ or CH_2Cl_2, ditopic structures **8** and **9**, respectively, were obtained in quantitative yields.

In the case of **8**, the self-assembly was monitored by means of ^1H NMR spectroscopy (see Supporting Information): By adding $[Pt(dppp)(OTf)_2]$ (0.5 equivalents) to a solution of cavitand **4** in CD_2Cl_2 (4:1 ratio), the only species present in solution were the free cavitand and the ditopic complex, with no evidence of partial-complexation products. After the addition of more metal precursor (0.5 equivalents, giving a 2:1 ligand/metal complex final ratio), only the ditopic cavitand complex **8** was present in solution. Addition of an excess of metal precursor left the self-assembled ditopic structure unchanged. The first coordinated cavitand facilitates the ligand entrance of the second, driving the reaction directly to the thermodynamically favored final product. Further evidence of the formation of self-assembled ditopic structures was obtained by means of electrospray ionization mass spectrometry (ESI-MS), which, in most cases, recorded prominent peaks at $m/z = [M-X]^+$ and $[M-2X]^{2+}$.

Crystals of **9** were grown by slow diffusion of absolute ethanol (EtOH) into a solution of **9** in CH_2Cl_2. The X-ray analysis clearly showed the presence of a dppp-chelated Pt center connecting two cavitands by coordination of the phenylpyridyl units in the *cis* position. The N-Pt-N bond angle was 86.9°, while the P-Pt-P angle was 91.1°, indicating a slight distortion of the square-planar geometry of the Pt center (Figure 2). In the solid state, the complex assumed a conformation with an approximate C_s symmetry. The two cavitands, almost related by a symmetry plane, were mutually rotated in such a way as to form an angle of about 90° between the two pseudo-fourfold axes passing through the cavities. The 19.3 Å distance between the centroids of the cavities (defined as the barycenter of the four Ar-CH-Ar methynic carbon atoms) evidenced the large dimensions of this class of ditopic complex. Each of the two cavities was filled with one ethanol molecule. In addition, two triflate counterions were located outside the cavity, one of these weakly coordinated to the metal by an oxygen atom (O–M = 4.0 Å). In the *trans* position to this triflate, a water molecule completes the very elongated octahedral arrangement of the metal ion (O–M = 4.0 Å).

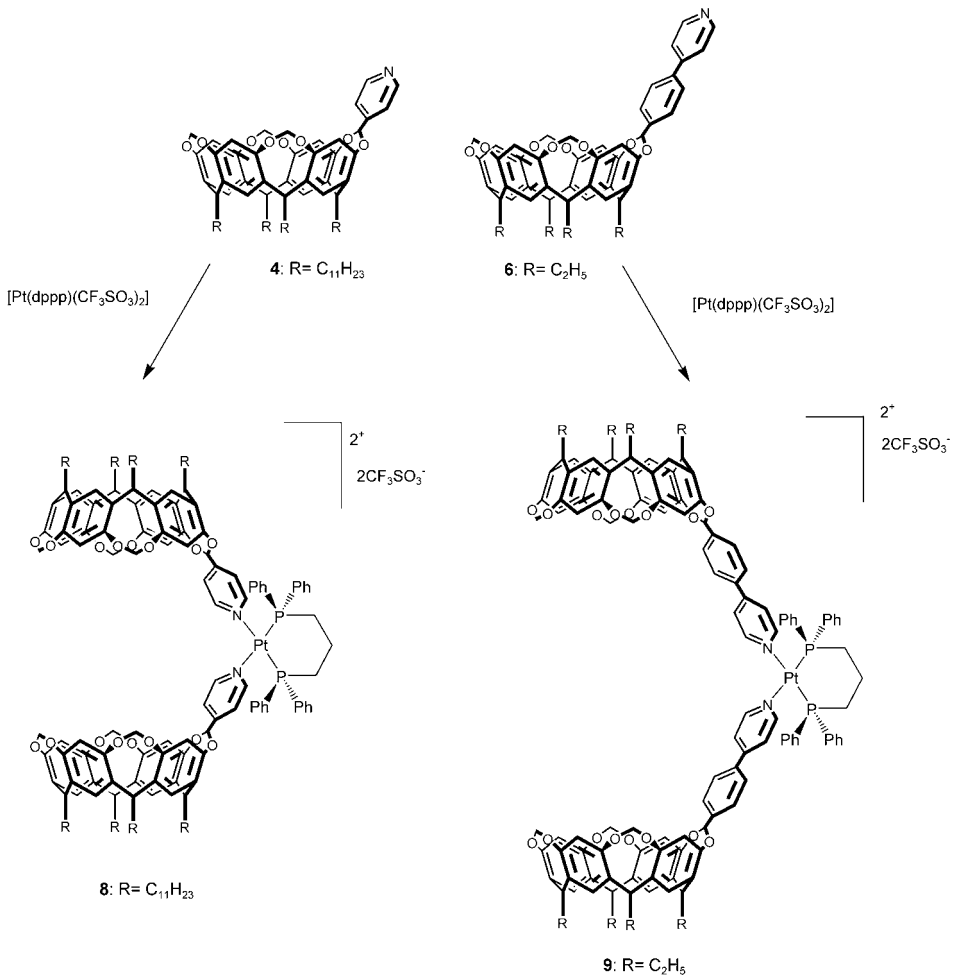

Scheme 2. Self-assembly of ditopic cavitands **8** and **9**.

Formation of kinetically inert, molecular ditopic complexes: The self-assembly protocol presented above leads to cavitand ditopic complexes with limited kinetic stability, due to the continuous formation/dissociation of these types of complexes in solution.[9] Due to the high *trans* effect of phosphine ligands, a different metal precursor must be employed when truly kinetically inert, ditopic cavitand complexes are desired. A possible solution relies on the use of Pt^{II} complexes that have ligands with a lower *trans* effect.

Our starting choice for the preparation of kinetically inert, ditopic complexes was to use the metal precursor *cis*-$[Pt(CH_3CN)_2Cl_2]$.[10] The proce-

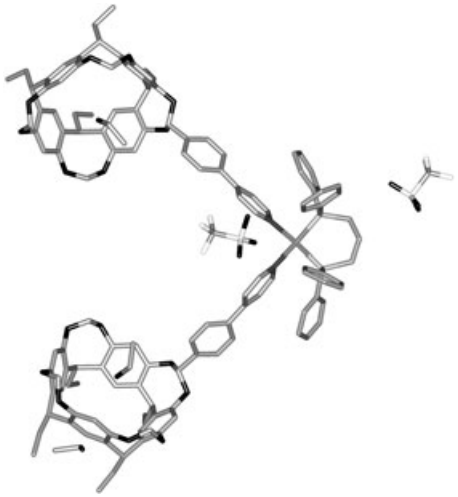

Figure 2. Crystal structure of ditopic cavitand complex **9**.

dure followed is shown in Scheme 3. In this case, under the reported conditions, both mono (**10**) and ditopic (**11**) complexes were obtained. However, it should be noted that starting with a metal precursor that has ligands with a low *trans* effect, the reaction rate significantly decreases with respect to the phosphine complexes. In fact, while the only products obtained in quantitative yields at room temperature from $[Pt(dppp)(OTf)_2]$ were the ditopic complexes, the exchange of the second CH_3CN ligand in *cis*-$[Pt(CH_3CN)_2Cl_2]$ was quite slow, and even after heating at 80 °C for several days 20 % of the monotopic derivative was still present. Both of the products, mono and ditopic complexes, were kinetically inert and were purified by silica-gel chromatography. ^1H NMR spectra showed the typical low-field shift of the pyridine hydrogen atoms indicative of coordination to the Pt center; these shifts were higher for the ditopic complexes than for the monotopic ones.

The stereochemistry of complexes **10** and **11** was determined by solving their crystal structures. Both complexes have the *cis–trans* isomerization of the chlorine ligands, with *trans* geometry formation of the cavitand ligands in the ditopic derivative **11**.

The crystal structure of **10** (Figure 3) shows that the monotopic complex forms a supramolecular dimer in the solid state, in which each methyl group of the residual acetonitrile ligand is inserted into the electron-rich cavity of the other cavitand complex. The crystal structure of *trans*-**11** (Figure 4) clearly shows that the two cavitand units are in a *trans* geometry. The two cavities are oriented in the opposite directions with one molecule of ethanol included in each cavity. The distance between the centroids of the cavities is 31.3 Å, quantifying the large size of this *trans* ditopic complex. An interesting feature of this crystal structure is the accentuated bow conformation of the complex as shown in Figure 4. This deviation from planarity reflects the flexibility of the phenylpyridyl moiety of the cavitand ligand.

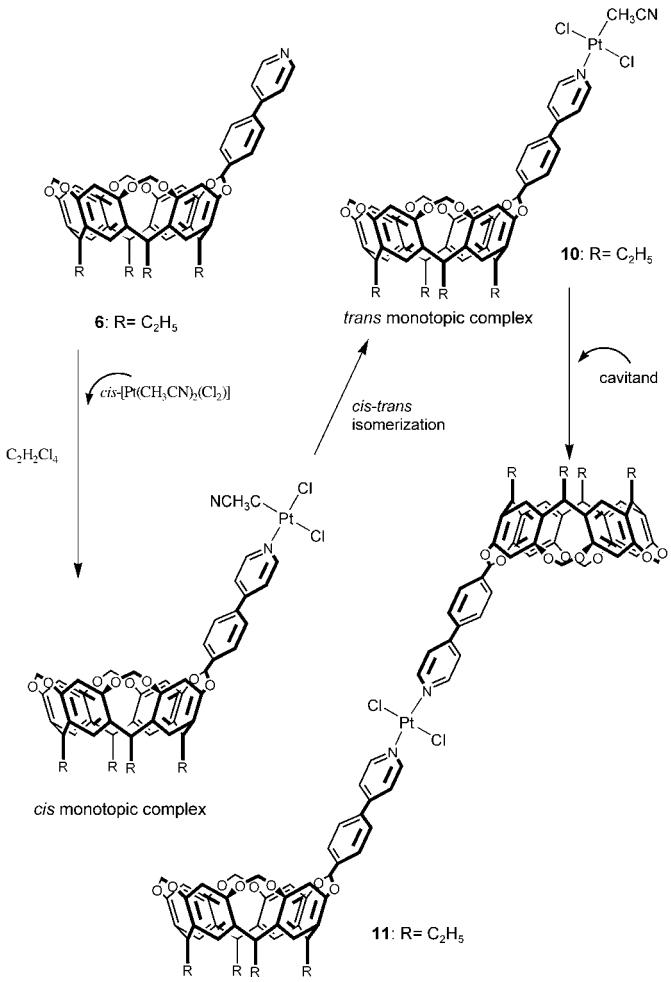

Scheme 3. Synthesis of mono and ditopic, respectively, phenylpyridyl cavitand complexes *trans*-**10** and *trans*-**11**, by using $[Pt(CH_3CN)_2Cl_2]$ as metal precursor.

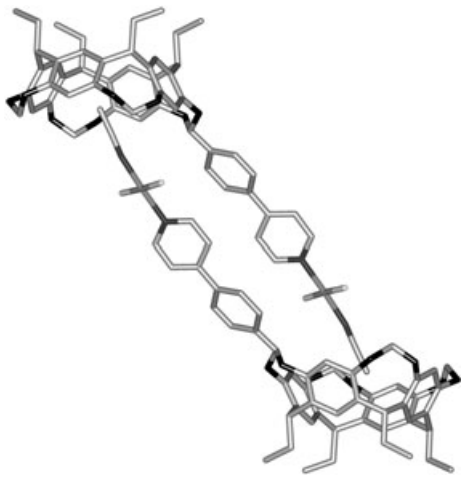

Figure 3. Crystal structure of monotopic cavitand complex *trans*-**10**.

The stereochemistry of the products can be explained by considering a *cis*-to-*trans* isomerization of the monofunctionalized cavitand complex (Scheme 3), as in the majority

Figure 4. Crystal structure of ditopic cavitand complex *trans*-**11**, obtained by the $[Pt(CH_3CN)_2Cl_2]$ route.

of reactions substitution at the Pt^{II} atom appears to proceed with retention of configuration. This equilibrium is totally shifted to the *trans* structure because no *cis* monotopic isomer is detected. The formation of dimeric species with mutual host–guest interactions, as suggested by the crystal structure, could be crucial in the stabilization of the *trans* isomer. Once the complex has changed its geometry, the second cavitand substitutes the remaining CH_3CN (in the *trans* position with respect to the previous one) quite slowly, as the pyridyl ligand has a low *trans* effect.[11]

To exclude the possibility of isomerization of the precursor itself by warming,[10] and to test if the *cis–trans* isomerization of the monotopic complex was favored by the temperature conditions of the reaction (80 °C), the experiment was repeated at room temperature. The same two products were obtained, with the only difference being the ratio between monotopic (**10**) and ditopic (**11**) complexes. At room temperature the monotopic product was obtained in higher yield than the ditopic one; while at 80 °C the result was completely reversed (see Experimental Section). Therefore, either the *cis–trans* isomerization of the monotopic complex is very fast and cannot be controlled under these experimental conditions, or the presence of specific host–guest interactions between acetonitrile Pt^{II} complexes and cavitands can protect the axial positions at the metal center, and the mechanism of substitution is no longer stereoretentive.

To avoid the *cis–trans* isomerization process and still have ditopic cavitand complexes that are kinetically inert, we resorted to a different Pt metal precursor, namely, *cis*-$[Pt(dmso)_2Cl_2]$, which is known to give exclusively *cis* supramolecular structures with pyridyl-substituted porphyrins.[12] The *cis*-$[Pt(dmso)_2Cl_2]$ complex was reacted with monophenylpyridyl cavitand **6**. The different reactivities of the two DMSO ligands allowed the reaction, at room temperature in CH_2Cl_2 for 4 h, to stop at the monosubstitution level. The product was isolated in quantitative yield (Scheme 4).

Despite the mild reaction conditions, both the *cis* and *trans* isomers were detected in solution by means of ^1H NMR spectroscopy. The spectrum showed two signals for the DMSO molecule: at 3.52 and 3.47 ppm, belonging to the

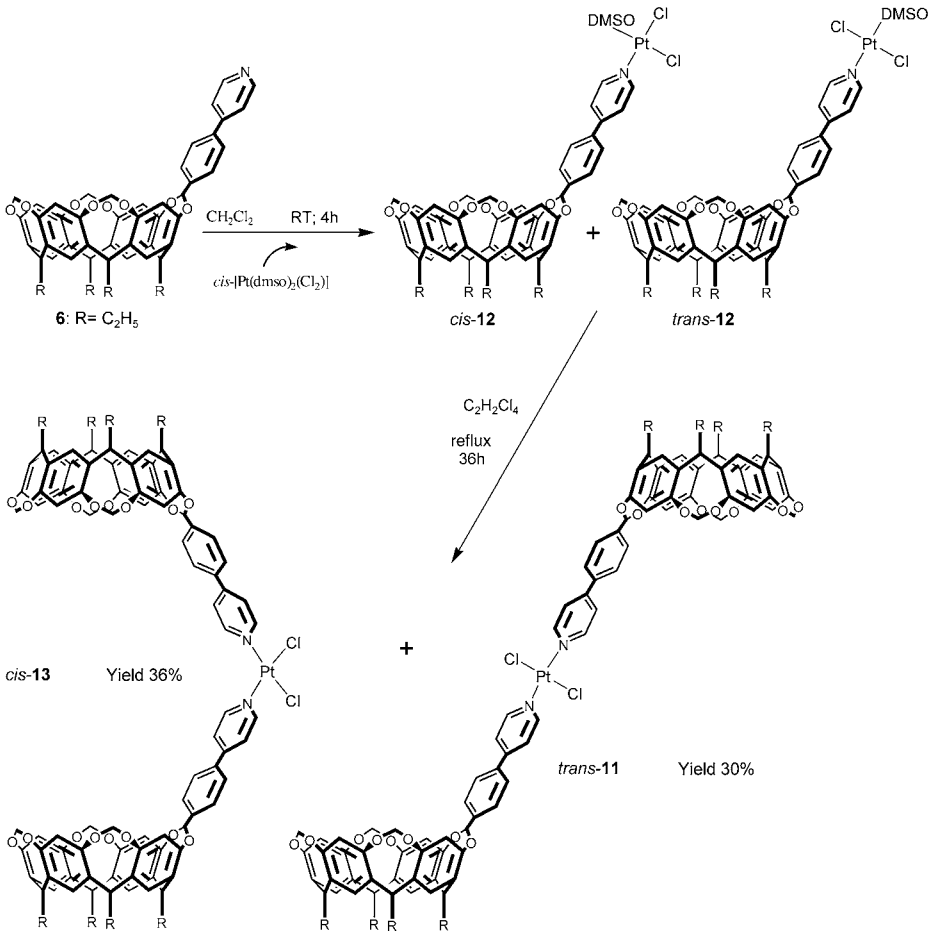

Scheme 4. Synthesis of monotopic *cis*- and *trans*-**12** and ditopic *cis*-**13** and *trans*-**11** phenylpyridyl cavitand complexes, by using $[Pt(dmso)_2Cl_2]$ as metal precursor. R = C_2H_5 for *cis*-**13** and *trans*-**11**.

cis and *trans* isomers, respectively.[13] The two isomers could not be separated by using standard silica-gel chromatography, therefore, we decided to proceed further in the complexation experiment towards the generation of ditopic complexes and isolate the two isomers at the final step. The *cis*/*trans* ratio was estimated by integration of the two DMSO peaks: a slight predominance of the *cis* isomer (1.2:1) was observed.

X-ray quality crystals of *trans*-**12** were obtained by dissolving the *cis*–*trans* mixture in CH_2Cl_2/EtOH (Figure 5). The crystal structure clearly shows that the remaining

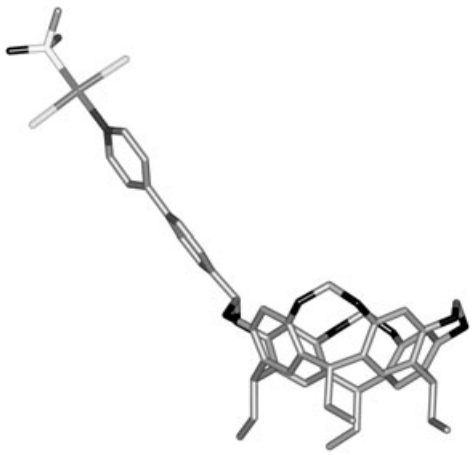

Figure 5. Crystal structure of monotopic cavitand complex *trans*-**12**.

DMSO ligand is coordinated to the Pt atom by the sulphur atom. Treatment of a *cis*/*trans* mixture of **12** with a second equivalent of cavitand **6** in refluxing $C_2H_2Cl_4$ resulted in the formation of both *cis*-**13** and *trans*-**11** ditopic cavitand complexes (Scheme 4). The two isomers were separated by silica-gel column chromatography. The **13**/**11** ratio remained the same as the starting *cis*/*trans* monotopic mixture ratio.

The attribution of the two isomers is based on the comparison of the spectral data of **13** with that of the *trans*-**11** isomer obtained with $[Pt(CH_3CN)_2Cl_2]$, determined from its crystal structure (Figure 4). ^{1}H NMR spectra indicated particular diagnostic signal differences in the aromatic pattern of the phenylpyridyl groups: $\delta(Py H_o) = 9.3$ ppm and $\delta(Py H_m) = 7.70$ ppm in **13,** versus 8.98 and 7.54 ppm, respectively, in **11**. The absence of visible satellites arising from the coupling with ^{195}Pt [^3J (^{195}Pt, ^{1}HPyH_o)] is due to chemical anisotropy relaxation, which makes them broad and less intense in high-field NMR instruments.[14] The attribution of **13** was further confirmed by MALDI-TOF analyses of **13** and **11**, in which the two complexes showed the same $[M+K]^+$ and $[M+Na]^+$ molecular ions.

X-ray-quality crystals were obtained by slow diffusion of absolute ethanol into a solution of **13** in CH_2Cl_2. Once more, the crystal structure (*trans*-**11**-bis) evidences that the two cavitand ligands are in a *trans* geometry in the complex (Figure 6). This surprising and unexpected result is explained by the presence of a slow *cis*–*trans* equilibrium in solution. Crystallization shifts the equilibrium towards the formation of the less soluble *trans*-**11** isomer. The ^{1}H NMR spectrum of the mother solution showed the presence of both isomers.

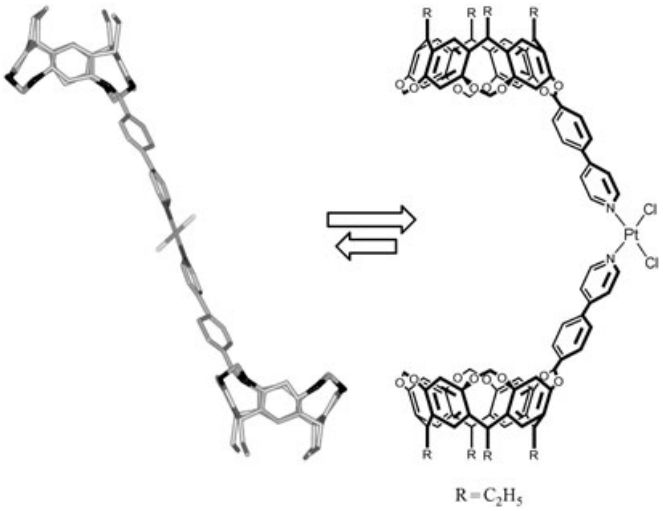

Figure 6. Crystal structure of ditopic complex *trans*-**11**, obtained by the $[Pt(dmso)_2Cl_2]$ route. The *cis*–*trans* equilibrium present in solution led to the exclusive formation of the *trans* isomer in the solid state.

The use of $[Pt(dmso)_2Cl_2]$ in place of $[Pt(CH_3CN)_2Cl_2]$ allowed the formation of the desired molecular ditopic complex *cis*-**13**. However, this synthetic procedure is not yet fully satisfactory because of the partial *cis*–*trans* isomerization in solution.

Self-assembly of a *fac*-Re ditopic complex: At this point we decided to change the coordinating metal, by changing to $[Re(CO)_5Br]$ as metal precursor. $[Re(CO)_5Br]$ is one of the few octahedral complexes that undergoes *cis* ligand exchange exclusively, due to the remarkable *trans* effect of carbonyl ligands. Typically, nitrogen ligands replace two equatorial *cis*-CO units of $[Re(CO)_5Br]$ to give neutral *fac*-$[Re(CO)_3L_2Br]$ complexes.[15]

Ditopic complex **14** was prepared by refluxing $[Re(CO)_5Br]$ and cavitand **6** in a 1:2.1 molar ratio (Scheme 5). A single product was isolated after purification by column chromatography. The ^{1}H NMR spectrum of this product was highly symmetric, showing the typical downfield shift of the pyridyl protons due to metal coordination. The $[M-Br]^+$ ion at $m/z = 1874$ was detected as molecular ion of complex **14** in the MALDI-TOF spectrum.

The stereochemistry of complex **14** was determined by monitoring the characteristic IR band maxima in the CO stretching region. The three-band pattern at 2029, 1928, and 1892 cm^{-1} was consistent with the *facial* arrangement of the three CO units in the coordination sphere.[16] The ^{13}C NMR spectrum was also consistent with the formation of the *fac*-**14** isomer; the spectrum showed the presence of a resonance at 191.9 ppm, typical of an axial CO unit.

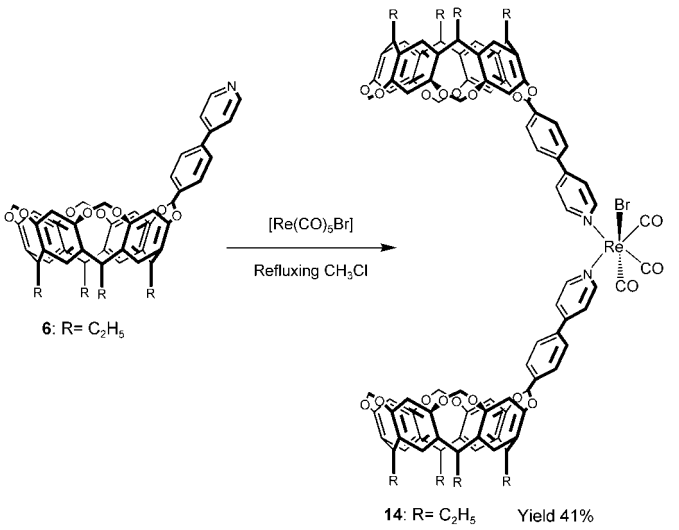

Scheme 5. Self-assembly of *fac*-Re ditopic cavitand complex **14**.

Based on the above results, the best protocol for the generation of kinetically inert, ditopic receptors was found to be this last one.

Self-assembly of tetratopic cavitand complexes: The formation of tetratopic cavitand complexes was a logical extension of the self-assembly procedure used for the ditopic ones. As a metal precursor, we selected a Pd complex in which all four ligands could be displaced by monopyridyl cavitands. $[Pd(CH_3CN)_4(BF_4)_2]$ was chosen, because its four labile CH_3CN groups can be easily replaced by pyridine ligands. The self-assembly process led to the quantitative formation of tetratopic cavitand complexes **15** and **16**, in which four cavitands are coordinated to the same metal center (Scheme 6). Both complexes were fully characterized by ^1H NMR spectroscopy and ESI-MS. They exhibited diagnostic downfield shifts of the protons in the α and β positions of the pyridine group upon coordination to Pd (see Supporting Information).

Complexes **15** and **16** were stable only in their mother solution. Removal of the solvent led to the formation of partially substituted complexes, in sharp contrast to the behavior of the corresponding ditopic complexes **8** and **9**. The instability of this class of tetratopic complex seems to be related to the presence of four, unconnected pyridyl ligands on the same metal,[11] and not to the bulkiness of the cavitand moiety: **16** behaved in the same way as **15**, despite the presence between the pyridyl and cavitand units of an aryl

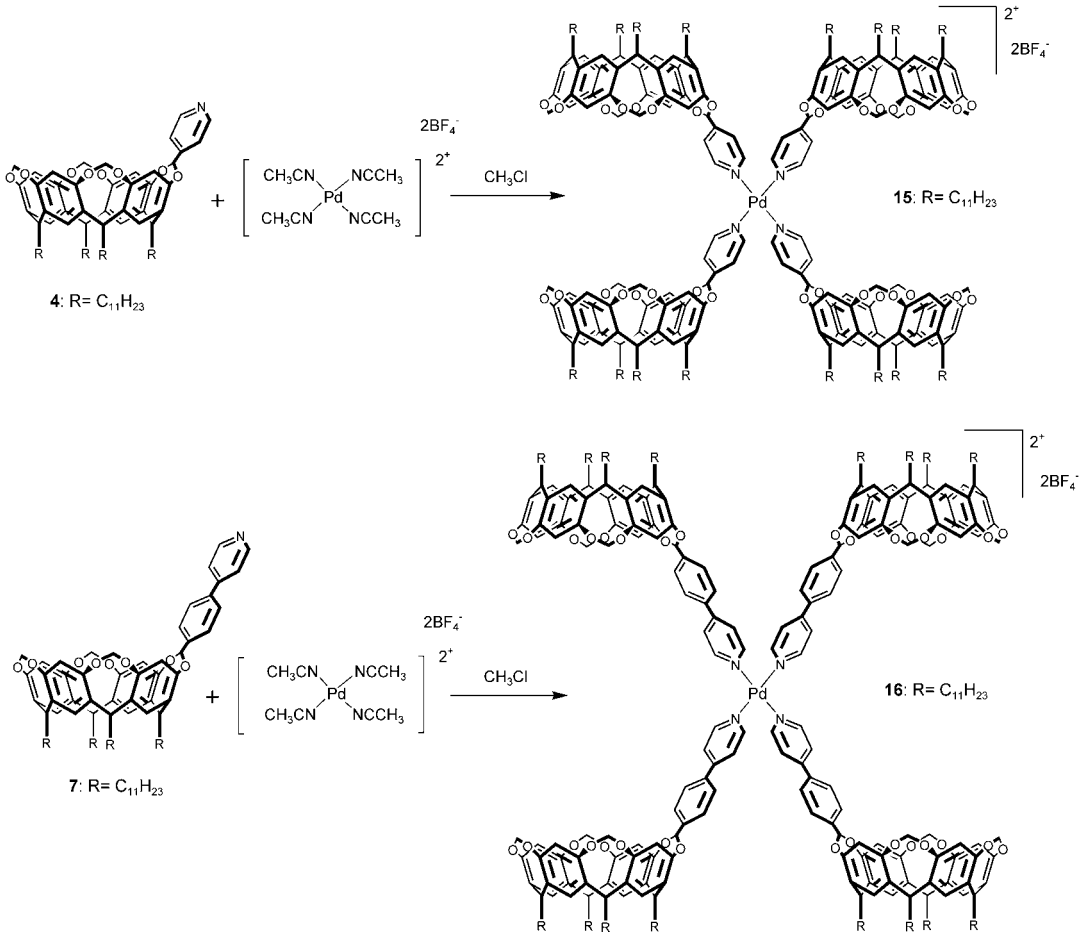

Scheme 6. Self-assembly of tetratopic cavitand complexes **15** and **16**.

spacer, which should reduce the steric congestion around the metal center. Stable Pd-tetrapyridine supramolecular complexes are known,[17] but only with chelating dipyridyl units. The different behavior found here led us to conclude that chelating ligands, such as dppp, are pivotal in providing chemical stability to square-planar Pt^{II} and Pd^{II} complexes. In this respect, a possible ligand for the metal precursor for the formation of tetratopic cavitand complexes is 1,2,4,5-tetrakis(diphenylphosphino)benzene (tppb).[18] This tetradentate chelating ligand can coordinate two metal ions, forming two equivalent square-planar complexes connected by a rigid phenyl spacer.

Metal precursors **19** and **20** were prepared by ligand exchange of *cis*-$[Pt(CH_3CN)_2Cl_2]$ and $[Pd(CH_3CN)_2Cl_2]$, respectively, with tppb, followed by reaction with $AgCF_3SO_3$ to introduce labile counterions.[19] These new dinuclear complexes were then tested in the self-assembly of tetratopic cavitand complexes. The first structure was obtained by mixing monopyridyl cavitand **3** and platinum complex **19** in a 4:1 ratio (Scheme 7). The reaction proceeded smoothly to give the desired complex **21** as the only product. The stability of the complex, both in solution and in the solid state, was excellent. The same protocol was applied to build the larger palladium complex **22**: monophenylpyridyl cavitand **6** and palladium spacer **20** were used as building blocks. Therefore, the ligand configuration at the metal centers, with two phosphorus and two cavitand ligands, was the most appropriate to build tetratopic cavitand complexes with sufficient kinetic stability.

Conclusions

In this work two different approaches to the preparation of ditopic cavitand complexes have been explored by using monodentate cavitand ligands as building blocks:

1) Self-assembly of ditopic complexes **8** and **9**. The desired ditopic complexes were obtained in quantitative yields by mixing the cavitand precursors with $[Pt(dppp)(OTf)_2]$ in a 1:2 ratio, following the well-established, cage self-assembly protocol.[8] The structural features of complex **9** were determined by means of X-ray crystallographic analysis of its crystals. The desired *cis* arrangement of the two cavitands was dictated by the chelating dppp ligand.
2) Formation of kinetically inert, molecular ditopic cavitand complexes by ligand-substitution reaction of appropriate neutral complexes. In this case three different routes were investigated: i) The use of *cis*-$[Pt(CH_3CN)_2Cl_2]$

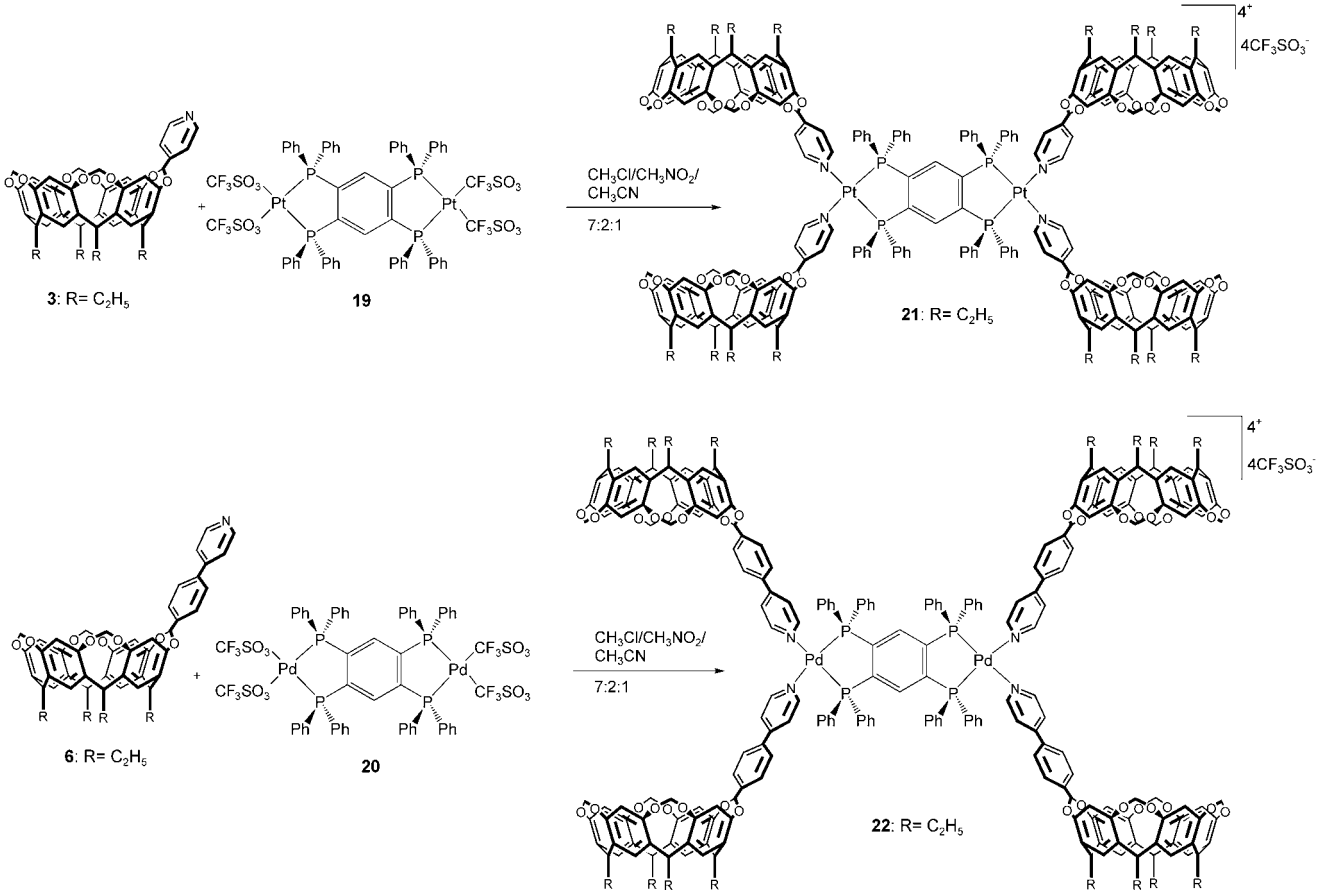

Scheme 7. Self-assembly of dinuclear tetratopic cavitand complexes **21** and **22**.

metal precursor led to the exclusive formation of mono *trans*-**10** and ditopic *trans*-**11** cavitand complexes. A complete *cis*-to-*trans* isomerization was observed after the coordination of the first cavitand ligand. ii) The use of *cis*-$[Pt(dmso)_2Cl_2]$ metal precursor led to partial *cis*-to-*trans* isomerization during the first ligand substitution. In this case, stepwise ligand substitution was made possible by the different reactivity of DMSO ligands. The desired *cis*-**13** ditopic complex was obtained, but it slowly isomerized to the corresponding *trans*-**11** one in solution. iii) The use of $[Re(CO)_5Br]$ metal precursor emerged as the best choice. The *trans* effect exerted by the equatorial CO ligands in the complex led to the desired substitution pathway. In this case the kinetically inert, *fac*-**14** complex with the *cis* arrangement of the two cavitand ligands was obtained as the single product.

As a result of this investigation, two different synthetic protocols for the preparation of ditopic cavitand complexes have been worked out. They have in common the exclusive formation of the desired complexes in the correct *cis* geometry, necessary for cooperative binding of ditopic guests. With these two procedures available, the next step will be to turn the cavitands into effective ligand receptors by replacing the three methylene bridges with appropriate moieties. The different kinetic stabilities of complexes **9** and **14** can be exploited under different working conditions: kinetically inert, neutral Re complexes can be used for complexation studies in solution, and the thermodynamic control over the formation of charged Pt complexes can be exploited in molecular recognition at the solid–liquid and solid-gas interfaces,[20] at which clean self-assembly on surfaces[21] is a necessary precondition.

The extension of the self-assembly protocol from ditopic complexes to tetratopic structures has been studied. Several different final structures have been envisaged, and their formation was tested in solution. The tetratopic mononuclear cavitand complexes **15** and **16** formed quantitatively under standard self-assembly conditions, but they were stable only in their mother solution. The use of dinuclear metal precursors **19** and **20** led to the self-assembly of tetratopic dinuclear cavitand complexes **21** and **22**, which were stable both in solution and in the solid state. The tppb ligands are therefore the spacers of choice for the generation of complex molecular architectures. The self-assembly behavior of monodentate cavitand ligands with different metal complexes is now fully predictable.

Experimental Section

General methods: All commercial reagents were ACS grade and used as received. All solvents were dried over 3 and 4 Å molecular sieves. ^{1}H NMR spectra were recorded on Bruker AC300 (300 MHz), Avance (300 MHz), and AMX400 (400 MHz) spectrometers and all chemical shifts (δ) were reported in parts per million (ppm) relative to the proton resonances resulting from incomplete deuteration of the NMR solvents. ^{13}C NMR spectra were recorded on a Brucker Avance (75 MHz) spectrometer. Melting points were obtained with an electrothermal capillary melting-point apparatus and were not corrected. Microanalyses were performed by using the facilities at Parma University. Mass spectra of the organic compounds were measured with a Finnigan MAT SSQ710 spectrometer, using the CI (chemical ionization) technique. Electrospray ionization mass spectrometry (ESI-MS) experiments were performed on a Waters ZMD spectrometer equipped with an electrospray interface. Matrix-assisted laser desorption ionization time-of-flight (MALDI-TOF) mass spectra were obtained on a PerSpective Biosystems Voyager DE-RP spectrometer equipped with delayed extraction. Column chromatography was performed by using silica gel 60 (Merck 70–230 mesh).

Resorcinarenes (R: C_2H_5; $C_{11}H_{23}$),[22] 4-(α,α′-dibromomethyl)pyridine,[8a] 4,4′-(α,α′-dibromo)tolylpyridine,[21b] *cis*-$[Pt(dmso)_2Cl_2]$,[23] and 1,2,4,5-tetrakis(diphenylphosphino)benzene (tppb)[18] were prepared according to literature procedures.

Ethyl-footed trimethylene-bridged resorcinarene (1): K_2CO_3 (5.53 g, 40 mmol) and CH_2Br_2 (0.77 mL, 11.0 mmol) were added, under nitrogen, to a solution of resorcinarene (R: C_2H_5) (3.0 g, 5.0 mmol) in dry DMSO (10 mL). The purple mixture was stirred in a sealed tube at 90 °C for 3 h. The reaction was quenched by the addition of HCl_{aq} (10 %), and the resulting mixture was extracted with CH_2Cl_2. The organic layer was washed with water (3×15 mL), dried on Na_2SO_4, and evaporated. The crude product was purified by column chromatography on silica gel by using CH_2Cl_2/ethyl acetate (7:3 v/v) as eluant to give resorcinarene **1** as a pale yellow solid (0.95 g, 1.15 mmol, 30 %). R_f=0.6; m.p. 260–265 °C; ^{1}H NMR (300 MHz, $CDCl_3$): δ=0.98 (m, 9H; CH_3), 1.26 (t, ^3J=7.1 Hz, 3H; CH_3), 2.26 (m, 8H; CHCH_2CH$_3$), 4.22 (t, ^3J=7.9 Hz, 1H; CHAr$_2$), 4.37 (d, ^2J=7.2 Hz, 1H; CH_{in}), 4.48 (d, ^2J=7.1 Hz, 2H; CH_{in}), 4.60 (t, ^3J=8.2 Hz, 1H; CHAr$_2$), 4.64 (t, ^3J=8.2 Hz, 2H; CHAr$_2$), 5.72 (d, ^2J=7.2 Hz, 1H; CH_{out}), 6.75 (d, ^2J=7.1 Hz, 2H; CH_{out}), 6.38 (s, 2H; ArH), 6.49 (s, 2H; ArH), 7.03 (br s, 2H; OH), 7.09 (s, 2H; ArH), 7.16 ppm (s, 2H; ArH); MS (CI): *m/z* (%): 637 (100) $[M+H]^+$.

Undecyl-footed trimethylene-bridged resorcinarene (2): K_2CO_3 (3.76 g, 27.2 mmol) and CH_2Br_2 (0.41 mL, 6.0 mmol) were added, under nitrogen, to a solution of resorcinarene (R: $C_{11}H_{23}$) (3.0 g, 2.72 mmol) in dry DMSO (10 mL). The purple mixture was stirred in a sealed tube at 90 °C for 3 h. The reaction was quenched by the addition of HCl_{aq} (10 %), and the resulting mixture was extracted with CH_2Cl_2. The organic layer was washed with water (3×15 mL), dried on Na_2SO_4, and evaporated. The crude product was purified by column chromatography on silica gel by using CH_2Cl_2/ethyl acetate (9:1 v/v) as eluant to give resorcinarene **2** as a pale yellow solid (1.1 g, 1.06 mmol, 39 %). R_f=0.62; m.p. 280–285 °C; ^{1}H NMR (300 MHz, $CDCl_3$): δ=0.88 (t, ^3J=6.4 Hz, 12H; CH_3), 1.27–1.40 (m, 72H; (CH_2)$_9$), 2.22 (m, 8H; CH(CH_2)R), 4.29 (t, ^3J=8.1 Hz, 1H; CHAr$_2$), 4.37 (d, ^2J=7.2 Hz, 1H; CH_{in}), 4.47 (d, ^2J=7.2 Hz, 2H; CH_{in}), 4.68 (t, ^3J=8.3 Hz, 1H; CHAr$_2$), 4.72 (t, ^3J=8.3 Hz, 1H; CHAr$_2$), 5.71 (d, ^2J=7.2 Hz, 1H; CH_{out}), 5.74 (d, ^2J=7.2 Hz, 2H; CH_{out}), 6.38 (s, 2H; ArH), 6.48 (s, 2H; ArH), 7.09 (s, 2H; ArH), 7.26 (s, 2H; ArH), 7.56 ppm (br s, 2H; OH); MS (CI): *m/z* (%): 1043 (100) $[M+H]^+$.

Ethyl-footed cavitand (3) ("out" isomer): 4-(α,α′-Dibromomethyl)pyridine (0.13 g, 0.39 mmol) and K_2CO_3 (0.9 g, 0.63 mmol) were added, under nitrogen, to a solution of resorcinarene **1** (0.1 g, 0.16 mmol) in dry DMA (15 mL). The mixture was stirred in a sealed tube at 80 °C for 16 h. The reaction was quenched by addition of water (10 mL), and the resulting mixture was extracted with CH_2Cl_2 (15 mL). The organic layer was washed with water (3×15 mL), dried on Na_2CO_3, and evaporated. The crude product was purified by column chromatography on silica gel by using CH_2Cl_2/hexane (7:3 v/v) as eluant to give compound **3** ("out" isomer) as a yellow solid (30 mg, 0.041 mmol, 26 %). The corresponding "in" isomer was not purified. R_f=0.35; m.p. 230 °C; ^{1}H NMR (300 MHz, $CDCl_3$): δ=1.00–1.06 (m, 12H; CH_3), 2.24–2.35 (m, 8H; CH_2-CH$_3$), 4.41 (d, ^2J=7.3 Hz, 1H; CH_{in}), 4.45 (d, ^2J=7.2 Hz, 2H; CH_{in}), 4.62–4.79 (m, 4H; CHAr$_2$), 5.42 (s, 1H; CHPy), 5.75 (d, ^2J=7.3 Hz, 1H; CH_{out}), 5.76 (d, ^2J=7.2 Hz, 2H; CH_{out}), 6.50 (s, 2H; ArH), 6.61 (s, 2H; ArH), 7.14 (s, 2H; ArH), 7.18 (s, 2H; ArH), 7.61 (m, (AA′ part of a AA′XX' system), 2H; PyH_m), 8.73 ppm (m, (XX′ part of a AA′XX' system), 2H; PyH_o); MS (CI): *m/z* (%): 725 (100) $[M+H]^+$.

Undecyl-footed cavitands (4) ("out" isomer) and (5) ("in" isomer): 4-(α,α′-Dibromomethyl)pyridine (0.15 g, 0.6 mmol) and K_2CO_3 (0.27 g, 1.93 mmol) were added, under nitrogen, to a solution of resorcinarene **2** (0.275 g, 0.24 mmol) in dry DMA (15 mL). The mixture was stirred in a sealed tube at 80 °C for 16 h. The reaction was quenched by addition of water (10 mL), and the resulting mixture was extracted with CH_2Cl_2 (15 mL). The organic layer was washed with water (3×15 mL), dried on Na_2CO_3, and evaporated. The crude product was purified by column chromatography on silica gel by using CH_2Cl_2/ethyl acetate (8:2 v/v) as eluant to give compound **4** ("out" isomer) as a yellow solid (90 mg, 0.073 mmol, 30 %) and compound **5** ("in" isomer) as a pale yellow solid (42 mg, 0.034 mmol, 14 %).

Data for 4 ("out" isomer): R_f=0.56; m.p. 220 °C; ^{1}H NMR (300 MHz, $CDCl_3$): δ=0.87 (t, ^3J=6.3 Hz, 12H; CH_3), 1.23–1.57 (m, 72H; $(CH_2)_9$), 2.24–2.29 (m, 8H; CHCH_2R), 4.40 (d, ^2J=7.2 Hz, 1H; CH_{in}), 4.44 (d, ^2J=7.2 Hz, 2H; CH_{in}), 4.75 (m, 3H; CHAr$_2$), 4.84 (t, ^3J=8.0 Hz, 1H; CHAr$_2$), 5.41 (s, 1H; CHPy), 5.74 (d, ^2J=7.2 Hz, 3H; CH_{out}), 5.75 (d, ^2J=7.2 Hz, 2H; CH_{out}), 6.48 (s, 2H; ArH), 6.60 (s, 2H; ArH), 7.13 (s, 2H; ArH), 7.17 (s, 2H; ArH), 7.60 (m, (AA′ part of a AA′XX' system), 2H; PyH_m), 8.71 ppm (m, (XX′ part of a AA′XX' system), 2H; PyH_o); ^{1}H NMR (300 MHz, CD_2Cl_2): δ=0.85 (t, ^3J=6.4 Hz, 12H; CH_3), 1.25–1.38 (m, 72H; $(CH_2)_9$), 2.25 (m, 8H; CHCH_2R), 4.30 (d, ^2J=7.2 Hz, 1H; CH_{in}), 4.35 (d, ^2J=7.2 Hz, 2H; CH_{in}), 4.74 (m, 3H; CHAr$_2$), 4.84 (t, ^3J=7.8 Hz, 1H; CHAr$_2$), 5.32 (s, 1H; CHPy), 5.71 (m, 2H; CH_{out}), 5.75 (d, ^2J=7.2 Hz, 2H; CH_{out}), 6.49 (s, 2H; ArH), 6.62 (s, 2H; ArH), 7.20 (s, 2H; ArH), 7.24 (s, 2H; ArH), 7.62 (m, (AA′ part of a AA′XX' system), 2H; PyH_m), 8.70 ppm (m, (XX′ part of a AA′XX' system), 2H; PyH_o); MS (CI): *m/z* (%): 1230 (100) $[M+H]^+$.

Data for 5 ("in" isomer): R_f=0.43; ^{1}H NMR (300 MHz, $CDCl_3$): δ=0.83 (t, ^3J=6.4 Hz, 12H; CH_3), 1.10–1.42 (m, 12H; $(CH_2)_9$), 2.16–2.40 (m, 8H; CHCH_2R), 3.76 (d, ^2J=7.3 Hz, 2H; CH_{in}), 4.30 (d, ^2J=7.3 Hz, 1H; CH_{in}), 4.75 (m, 4H; CHAr$_2$), 5.53 (d, ^2J=7.3 Hz, 2H; CH_{out}), 5.80 (s, 2H; ArH), 5.81 (d, ^2J=7.3 Hz, 1H; CH_{out}), 6.48 (s, 2H; ArH), 6.60 (s, 1H; CHPy), 7.14 (m, (AA′ part of a AA′XX' system), 2H; PyH_m), 7.20 (s, 2H; ArH), 7.21 (s, 2H; ArH), 7.51 ppm (brs, (XX′ part of a AA′XX' system), 2H; PyH_o); MS (CI): *m/z* (%): 1230 (100) $[M+H]^+$.

Ethyl-footed cavitand (6) ("out" isomer): 4,4′-(α,α′-Dibromo)tolylpyridine (0.23 g, 0.69 mmol) and K_2CO_3 (0.35 g, 2.56 mmol) were added, under nitrogen, to a solution of resorcinarene **1** (0.22 g, 0.35 mmol) in dry DMA (10 mL). The mixture was stirred in a sealed tube at 80 °C for 16 h. The reaction was quenched by addition of water (10 mL), and the resulting mixture was extracted with CH_2Cl_2 (15 mL). The organic layer was washed with water (3×15 mL), dried on Na_2CO_3, and evaporated. The crude product was purified by column chromatography on silica gel by using CH_2Cl_2/ethyl acetate (6:4 v/v) as eluant to give compound **6** ("out" isomer) as a white solid (0.13 g, 0.16 mmol, 46 %). R_f=0.45; m.p. 220 °C; ^{1}H NMR (300 MHz, $CDCl_3$): δ=1.01–1.07 (m, 12H; CH_3), 2.25–2.36 (m, 8H; CH_2-CH$_3$), 4.42 (d, ^2J=7.2 Hz, 1H; CH_{in}) 4.46 (d, ^2J=7.2 Hz, 2H; CH_{in}), 4.64–4.81 (m, 4H; CHAr$_2$), 5.52 (s, 1H; CHPhPy), 5.76 (d, ^2J=7.2 Hz, 1H; CH_{out}), 5.77 (d, ^2J=7.2 Hz, 2H; CH_{out}), 6.50 (s, 2H; ArH), 6.62 (s, 2H; ArH), 7.14 (s, 2H; ArH), 7.21 (s, 2H; ArH), 7.52 (d, ^3J=5.8 Hz, (AA′ part of a AA′XX′ system), 2H; PyH_m), 7.71 (d, J_o=6.5 Hz, J_m=2.1 Hz, (AA′ part of a AA′XX′ system), 2H; PyPhH), 7.82 (d, J_o=6.5 Hz, J_m=2.1 Hz, (XX′ part of a AA′XX′ system), 2H; PyPhH), 8.69 ppm (d, ^3J=5.8 Hz, (XX′ part of a AA′XX′ system), 2H; PyH_o); ^{1}H NMR (300 MHz, CD_2Cl_2): δ=0.98–1.04 (m, 12H; CH_3), 2.23–2.35 (m, 8H; CH_2-CH$_3$), 4.33 (d, ^2J=7.2 Hz, 1H; CH_{in}) 4.38 (d, ^2J=7.2 Hz, 2H; CH_{in}), 4.64(m, 3H; CHAr$_2$), 4.80 (t, ^3J=8.0 Hz, 1H; CHAr$_2$), 5.44 (s, 1H; CHPhPy), 5.73 (d, ^2J=7.2 Hz, 1H; CH_{out}), 5.75 (d, ^2J=7.2 Hz, 2H; CH_{out}), 6.50 (s, 2H; ArH), 6.66 (s, 2H; ArH), 7.24 (s, 2H; ArH), 7.20 (s, 2H; ArH), 7.57 (d, ^3J=6.0 Hz, (AA′ part of a AA′XX′ system), 2H; PyH_m), 7.76 (d, J_o=6.5 Hz, J_m=2.1 Hz, (AA′ part of a AA′XX′ system), 2H; PyPhH), 7.85 (d, J_o=6.5 Hz, J_m=2.1 Hz, (XX′ part of a AA′XX′ system), 2H; PyPhH), 8.67 ppm (d, J=5.8 Hz, (XX′ part of a AA′XX′ system), 2H; PyH_o); MS (CI): *m/z* (%): 802 (100) $[M+H]^+$.

Undecyl-footed cavitand (7) ("out" isomer): 4,4′-(α,α′-Dibromo)tolylpyridine (0.46 g, 1.4 mmol) and K_2CO_3 (0.62 g, 4.5 mmol) were added, under nitrogen, to a solution of resorcinarene **2** (0.64 g 0.56 mmol) in dry DMA (15 mL). The mixture was stirred in a sealed tube at 80 °C for 16 h. The reaction was quenched by addition of water (10 mL), and the resulting mixture was extracted with CH_2Cl_2 (15 mL). The organic layer was washed with water (3×15 mL), dried on Na_2CO_3, and evaporated. The crude product was purified by column chromatography on silica gel using CH_2Cl_2/ethyl acetate (3:7 v/v) as eluant to give compound **7** ("out" isomer) as a pale yellow solid (0.40 g, 0.30 mmol, 54 %). R_f=0.57; m.p. 225 °C; ^{1}H NMR (300 MHz, $CDCl_3$): δ=0.87 (t, ^3J=6.4 Hz, 12H; CH_3), 1.22–1.41 (m, 72H; $(CH_2)_9$), 2.26 (m, 8H; CHCH_2R), 4.43 (d, ^2J=7.3 Hz, 1H; CH_{in}), 4.47 (d, ^2J=7.2 Hz, 2H; CH_{in}), 4.75 (m, 2H; CHAr$_2$), 4.90 (t, ^3J=8.1 Hz, 1H; CHAr$_2$), 5.50 (s, 1H; CHPhPy), 5.75 (d, ^2J=7.3 Hz, 1H; CH_{out}), 5.76 (d, ^2J=7.2 Hz, 2H; CH_{out}), 6.50 (s, 2H; ArH), 6.63 (s, 2H; ArH), 7.14 (s, 2H; ArH), 7.18 (s, 2H; ArH), 7.53 (d, ^3J=5.9 Hz, (AA′ part of a AA′XX′ system), 2H; PyH_m), 7.72 (d, ^3J=8.3 Hz, (AA′ part of a AA′XX′ system), 2H; PyPhH), 7.81 (d, ^3J=8.3 Hz, (XX′ part of a AA′XX′ system), 2H; PyPhH), 8.68 ppm (d, J=5.7 Hz, (XX′ part of a AA′XX′ system), 2H; PyH_o); MS (CI): *m/z* (%): 1308 (100) $[M+H]^+$.

General procedure for the self-assembly of *cis*-ditopic cavitand complexes (8, 9): Ditopic complexes **8** and **9** were assembled by simply mixing, respectively, cavitands **4** or **6** with $[Pt(dppp)(OTf)_2]$ in a 2:1 molar ratio at room temperature in solvents such as CH_2Cl_2 or $CHCl_3$. In all cases, removal of the solvent under vacuum gave the desired complex as the only product in quantitative yields.

Data for 8: ^{1}H NMR (300 MHz, CD_2Cl_2): δ=0.87 (m, 24H; CH_3), 1.23–1.57 (m, 144H; $(CH_2)_9$), 2.16–2.26 (m, 2H; PCH$_2$CH_2CH$_2$), 2.24–2.29 [m, 16H; CHCH_2R], 3.36 (brm, 4H; PCH_2CH$_2$), 4.25 (d, ^2J=7.4 Hz, 2H; CH_{in}), 4.29 (d, ^2J=7.3 Hz, 4H; CH_{in}), 4.71 (m, 8H; CHAr$_2$), 5.07 (s, 2H; CHPy), 5.70 (d, ^2J=7.3 Hz, 4H; CH_{out}), 5.72 (d, ^2J=7.4 Hz, 2H; CH_{out}), 6.41 (s, 4H; ArH), 6.46 (s, 4H; ArH), 7.15 (s, 4H; ArH), 7.18 (s, 4H; ArH), 7.37 (m, 40H; Ph), 7.71 (brs, (AA′ part of a AA′XX′ system), 4H; PyH_m), 9.14 ppm (d, ^3J=5.2 Hz, (XX′ part of a AA′XX′ system), 4H; PyH_o); ESI-MS: *m/z* (%): calcd for $C_{191}H_{256}F_6N_2O_{22}P_2PtS_2$ (3367.3 amu) $[M-CF_3SO_3]^+$: 3218.1; found: 3218 (10); calcd $[M-2CF_3SO_3]^{2+}$: 1534.5; found: 1534 (100).

Data for 9: ^{1}H NMR (300 MHz, CD_2Cl_2): δ=1.03 (m, 24H; CH_3), 2.27–2.37 (m, 16H; CH_2-CH$_3$), 3.34 (brm, 16H; PCH_2CH$_2$), 4.31 (d, ^2J=7.4 Hz, 2H; CH_{in}), 4.34 (d, ^2J=7.3 Hz, 4H; CH_{in}), 4.64 (m, 6H; CHAr$_2$), 4.76 (t, ^3J=8.0 Hz, 2H; ArH), 5.38 (s, 2H; CH_{in}PhPy), 5.73 (d, ^2J=7.3 Hz, 6H; CH_{out}), 6.49 (s, 4H; ArH), 6.62 (s, 4H; ArH), 7.19 (s, 4H; ArH), 7.23 (s, 4H; ArH), 7.34 (d, ^3J=6.1 Hz, (AA′ part of a AA′XX′ system), 4H; PyPhH), 7.37 (m, 40H; PPh), 7.52 (d, ^3J=8.2 Hz, (AA′ part of a AA′XX′ system), 4H; PyPhH), 7.74–7.80 (brs, (AA′ part of a AA′XX′ system), 4H; PyH_m), 9.08 ppm (brd, (XX′ part of a AA′XX′ system), 4H; PyH_o); ESI-MS: *m/z* (%): calcd for $C_{131}H_{120}F_6N_2O_{22}P_2PtS_2$ (2509.5 amu) $[M-CF_3SO_3]^+$: 2360.5; found: 2361 (30); calcd $[M-2CF_3SO_3]^{2+}$: 1105.7; found: 1106 (100).

Mono (*trans*-10) and ditopic (*trans*-11) cavitand complexes: Ditopic *trans*-$PtCl_2$ cavitand complex **11** was prepared by mixing a solution of cavitand **6** in $C_2H_2Cl_4$ with *cis*-$[Pt(CH_3CN)_2Cl_2]$ in CH_3CN (2:1 molar ratio). The mixture was stirred at 80 °C for 3 days. After solvent evaporation, the crude yellow product was purified by column chromatography on silica gel using CH_2Cl_2/ethanol (98:2 v/v) as eluant to give the ditopic cavitand complex *trans*-**11** (50 %) and the monofunctionalized $PtCl_2$ cavitand complex *trans*-**10** (20 %). The same reaction carried out at room temperature gave **10** and **11** in 75 % and 17 % yields, respectively.

Data for 10: ^{1}H NMR (300 MHz, $CDCl_3$): δ=1.01 (m, 12H; CH_3), 2.17 (s, 3H; CH_3CN), 2.29 (m, 8H; CH_2-CH$_3$), 4.42 (d, ^2J=7.1 Hz, 1H; CH_{in}) 4.46 (d, ^2J=7.2 Hz, 2H; CH_{in}), 4.66, 4.81 (m, 4H; CHAr$_2$), 5.50 (s, 1H; CHPhPy), 5.75 (d, ^2J=7.1 Hz, 3H; CH_{out}), 6.50 (s, 2H; ArH), 6.61 (s, 2H; ArH), 7.14 (s, 2H; ArH), 7.18 (s, 2H; ArH), 7.55 (d, ^3J=6.0 Hz, (AA′ part of a AA′XX′ system), 2H; PyH_m), 7.69 (d, ^3J=8.2 Hz, (AA′ part of a AA′XX′ system), 2H; PyPhH), 7.83 (d, ^3J=8.2 Hz, (XX′ part of a AA′XX′ system), 2H; PyPhH), 8.84 ppm (d, ^3J=6.0 Hz, (XX′ part of a AA′XX′ system), 2H; PyH_o); MALDI-TOF MS: *m/z* (%): calcd for $C_{53}H_{50}Cl_2O_8N_2Pt$ (1108.9 amu) $[M+H]^+$: 1109.9; found: 1110 (60); calcd $[M+Na]^+$: 1131.9; found: 1133 (100).

Data for 11: ^{1}H NMR (300 MHz, $CDCl_3$): δ=1.03 (m, 24H; CH_3), 2.29 (m, 16H; CH_2-CH$_3$), 4.42 (d, ^2J=7.1 Hz, 2H; CH_{in}) 4.46 (d, ^2J=7.2 Hz,

4H; CH_{in}), 4.66, 4.81 (m, 8H; CHAr$_2$), 5.51 (s, 2H; CHPhPy), 5.76 (d, ^2J=7.1 Hz, 6H; CH_{out}), 6.50 (s, 4H; ArH), 6.61 (s, 4H; ArH), 7.15 (s, 4H; ArH), 7.19 (s, 4H; ArH), 7.54 (d, ^3J=6.6 Hz, (AA′ part of a AA′XX′ system), 4H; PyH_m), 7.72 (d, ^3J=8.0 Hz, (AA′ part of a AA′XX′ system), 4H; PyPhH), 7.84 (d, ^3J=8.0 Hz, (XX′ part of a AA′XX′ system), 4H; PyPhH), 8.97 ppm (d, ^3J=6.6 Hz, (XX′ part of a AA′XX′ system), 4H; PyH_o); MALDI-TOF MS: *m/z* (%): calcd for $C_{102}H_{94}Cl_2N_2O_{16}Pt$ (1869.9 amu) [M+Na]$^+$: 1892.8; found: 1892 (80); calcd [M+K]$^+$: 1909.0; found 1908.6 (20).

Monotopic cavitand complexes (*cis*+*trans*-12): A solution of cavitand **6** (110 mg, 0.137 mmol) and *cis*-[Pt(dmso)$_2$Cl$_2$] (58 mg, 0.137 mmol) in CH_2Cl_2 (10 mL) was stirred at room temperature in the dark for 4 h. The solvent was removed under vacuum to give monotopic *cis*+*trans*-**12** complex in quantitative yield. The two isomers could not be separated chromatographically. The experimental *cis*/*trans* ratio was 1.2:1, obtained by integration of the 3.52 and 3.47 ppm DMSO singlets. *cis*+*trans*-**12**: ^{1}H NMR (300 MHz, $CDCl_3$): δ=1.03 (m, 12H; CH_3), 2.30 (m, 8H; CH_2CH$_3$), 3.47 (s, 6H; *trans*-DMSO), 3.52 (s, 6H; *cis*-DMSO), 4.42 (d, ^2J=7.2 Hz, 1H; CH_{in}) 4.47 (d, ^2J=7.2 Hz, 2H; CH_{in}), 4.66 (m, 3H; CHAr$_2$), 4.79 (t, ^3J=8.1 Hz, 1H; CHAr$_2$), 5.50 (s, 1H; CHPhPy), 5.73 (d, ^2J=7.2 Hz, 1H; CH_{out}), 5.75 (d, ^2J=7.2 Hz, 2H; CH_{out}), 6.50 (s, 2H; ArH), 6.62 (s, 2H; ArH), 7.13 (s, 2H; ArH), 7.18 (s, 2H; ArH), 7.63 (d, ^3J=6.8 Hz, (AA′ part of a AA′XX′ system), 2H; PyH_m), 7.71 (d, ^3J=8.4 Hz, (AA′ part of a AA′XX′ system), 2H; PyPhH), 7.83 (d, ^3J=8.4 Hz, (XX′ part of a AA′XX′ system), 2H; PyPhH), 8.78 ppm (d, ^3J=6.8 Hz, (XX′ part of a AA′XX′ system), 2H; PyH_o); MALDI-TOF MS: *m/z* (%): calcd for $C_{53}H_{53}Cl_2NO_9PtS$ (1146.0 amu) [M+Na]$^+$: 1169.0; found: 1169 (70); calcd [M+K]$^+$: 1185.1; found: 1185 (100).

***cis*-PtCl$_2$ ditopic complex (13)**: Cavitand **6** (45 mg, 0.056 mmol) was added to a $C_2H_2Cl_4$ solution of *cis*+*trans*-**12** complexes (77 mg, 0.056 mmol). The solution was heated to reflux for 36 h. The solvent was removed under vacuum, and the crude mixture was purified by column chromatography on silica gel using $CHCl_3$/ethyl acetate (95:5 v/v) as eluant to give **13** (38 mg, 0.02 mmol, 36%) and **11** (31 mg, 0.17 mmol, 30%).

Data for 13: ^{1}H NMR (300 MHz, $CDCl_3$): δ=1.04 (m, 24H; CH_3), 2.32 (m, 16H; CH_2CH$_3$), 4.44 (d, ^2J=7.1 Hz, 2H; CH_{in}), 4.48 (d, ^2J=7.1 Hz, 4H; CH_{in}), 4.68 (m, 6H; CHAr$_2$), 4.80 (t, ^3J=8.1 Hz, 2H; CHAr$_2$), 5.52 (s, 2H; CHPhPy), 5.76 (m, 6H; CH_{out}), 6.51 (s, 4H; ArH), 6.64 (s, 4H; ArH), 7.15 (s, 4H; ArH), 7.20 (s, 4H; ArH), 7.70 (d, ^3J=7.1 Hz, (AA′ part of a AA′XX′ system), 2H; PyH_m), 7.77 (d, ^3J=8.5 Hz, (AA′ part of a AA′XX′ system), 4H; PyPhH_m), 7.90 (d, ^3J=8.3 Hz, (XX′ part of a AA′XX′ system), 4H; PyPhH), 9.29 ppm (d, ^3J=7.1 Hz, (XX′ part of a AA′XX′ system), 4H; PyH_o); MALDI-TOF MS**:** *m/z* (%): calcd for $C_{102}H_{94}Cl_2N_2O_{16}Pt$ (1869.9 amu) [M+Na]$^+$: 1892.8; found: 1892 (20); calcd [M+K]$^+$: 1909.0; found: 1911 (100).

***fac*-Re ditopic cavitand complex (14)**: Cavitand **6** (48.1 mg, 0.06 mmol) was added to a $CHCl_3$ solution of [Re(CO)$_5$Br] (12.2 mg, 0.03 mmol) and heated to reflux for 24 h. After solvent evaporation, the crude product was purified by column chromatography on silica gel using CH_2Cl_2/ethanol (99:1 v/v) as eluant to give the ditopic cavitand complex *fac*-**14** (24.0 mg, 0.012 mmol, 41%). ^{1}H NMR (300 MHz, $CDCl_3$): δ=0.88 (m, 24H; CH_3), 2.30 (m, 16H; CH_2-CH$_3$), 4.41 (d, ^2J=7.2 Hz, 2H; CH_{in}) 4.45 (d, ^2J=7.2 Hz, 4H; CH_{in}), 4.64 (m, 6H; CHAr$_2$), 4.78 (t, ^3J=8.1 Hz, 2H; CHAr$_2$), 5.50 (s, 2H; CHPhPy), 5.74 (d, ^2J=7.2 Hz, 6H; CH_{out}), 6.49 (s, 4H; ArH), 6.61 (s, 4H; ArH), 7.13 (s, 4H; ArH), 7.18 (s, 4H; ArH), 7.59 (d, ^3J=6.6 Hz, (AA′ part of a AA′XX′ system), 4H; PyH_m), 7.70 (d, ^3J=8.3 Hz, (AA′ part of a AA′XX′ system), 4H; PyPhH), 7.84 (d, ^3J=8.3 Hz, (XX′ part of a AA′XX′ system), 4H; PyPhH), 8.90 ppm (d, ^3J=6.6 Hz, (XX′ part of a AA′XX′ system), 4H; PyH_o); ^{13}C NMR (75 MHz, $CDCl_3$): δ=12.2 (CH$_3$), 29.6 (CH$_2$), 38.2 (CH), 99.5 (OCH$_2$O), 106.8 (CHPhPy), 116.4 (CH), 120.6 (CH), 120.8 (CH), 123.2 (CH), 127.1 (CH), 127.4 (CH), 136.6 (Cq), 138.2 (Cq), 138.9 (Cq), 140.6 (Cq), 150 (Cq), 153.8 (CH), 154.8 (CH), 191.9 (CO$_{ax}$), 195 ppm (CO$_{eq}$); FTIR: ν_{CO}= 2029, 1929, 1892 cm^{-1}; MALDI-TOF MS: *m/z* (%): calcd for $C_{105}H_{94}BrN_2O_{19}Re$ (1954.0 amu) [M−Br]$^+$: 1874.1; found: 1874 (100).

General procedure for the self-assembly of mononuclear tetratopic cavitand complexes (15, 16): The tetratopic mononuclear cavitand complexes **15** and **16** were assembled by mixing cavitands **4** and **7,** respectively, with [Pd(CH$_3$CN)$_4$(BF$_4$)$_2$] in a 4:1 molar ratio at room temperature in a mixture of $CHCl_3$/CH_3CN (8:2). The complexes were stable only in the mother solution. All attempts to obtain them in the solid state, either by evaporation of the solvent or by precipitation, failed.

Data for 15: ^{1}H NMR (400 MHz, $CDCl_3$/CD_3CN): δ=1.16 (m, 48H; CH_3), 2.25 (m, 32H; CHCH_2CH$_3$), 4.35 (d, ^2J=7.2 Hz, 12H; CH_{in}), 4.61 (m, 16H; CHAr$_2$), 5.35 (s, 4H; CHPy), 5.69 (m, 12H; CH_{out}), 6.46 (s, 8H; ArH), 6.52 (s, 8H; ArH), 7.10 (s, 8H; ArH), 7.15 (s, 8H; ArH), 7.80 (d, ^3J=6.2 Hz, (AA′ part of a AA′XX′ system), 8H; PyH_m), 9.45 ppm (d, ^3J=6.2 Hz (XX′ part of a AA′XX′ system), 8H; PyH_o); ESI-MS: *m/z* (%): calcd for $C_{180}H_{172}B_2F_8N_4O_{32}Pd$ (3183.6 amu) [M−BF$_4$]$^+$: 3096.8; found: 3095 (10);, calcd [M−2BF$_4$]$^{2+}$: 1505.0; found: 1504 (100).

Data for 16: ^{1}H NMR (400 MHz, $CDCl_3$/CD_3CN): δ=0.87 (m, 48H; CH_3), 1.28–1.44 [m, 288H; (CH_2)$_9$], 2.26 (m, 32H; CHCH_2R), 4.36 (m, 12H; CH_{in}), 4.70 (m, 12H; CHAr$_2$), 4.81 (t, ^3J=7.8 Hz, 4H; CHAr$_2$), 5.40 (s, 4H; CHPhPy), 5.69 (d, ^2J=7.3 Hz, 12H; CH_{out}), 6.46 (s, 8H; ArH), 6.56 (s, 8H; ArH), 7.13 (s, 8H; ArH), 7.17 (s, 8H; ArH), 7.63 (d, ^3J=8.3 Hz, (AA′ part of a AA′XX′ system), 8H; PyPhH), 7.71 (d, ^3J= 5.8 Hz, (AA′ part of a AA′XX′ system), 8H; PyH_m), 7.76 (d, ^3J=8.3 Hz, (XX′ part of a AA′XX′ system), 8H; PyPhH), 9.37 ppm (d, ^3J=5.8 Hz, (XX′ part of a AA′XX′ system), 8H; PyH_o); ESI-MS: *m/z* (%): calcd for $C_{348}H_{476}B_2F_8N_4O_{32}Pd$ (5507.8 amu) [M−2BF$_4$]$^{2+}$: 2667.1; found: 2668 (80).

[Pt$_2$(tppb)Cl$_4$] (17): *cis*-[Pt(CH$_3$CN)$_2$Cl$_2$] (219.1 mg, 0.63 mmol) was added, under nitrogen, to a solution of tppb (256 mg, 0.31 mmol) in dry CH_3CN (15 mL) and dry CH_2Cl_2 (15 mL). The white solution was stirred at room temperature in the dark overnight. The solvent was removed under reduced pressure and the complex **17** (350 mg, 0.26 mmol, 82%) was purified by crystallization from ethyl ether. ^{1}H NMR (400 MHz, [D$_6$]DMSO): δ=7.51 (m, 16H; PPhH_o), 7.59 (t, ^3J=6.0 Hz, 8H; PPhH_p), 7.72 (m, 16H; PPhH_m), 8.01 ppm (brs, 2H; ArH); MALDI-TOF MS: *m/z* (%): calcd for $C_{54}H_{42}Cl_4P_4Pt_2$ (1346.8 amu) [M−Cl]$^+$: 1311.3; found: 1310 (100); calcd [M+Na]$^+$: 1369.8; found: 1369 (20); elemental analysis calcd (%) for $C_{54}H_{42}Cl_4P_4Pt_2$: C 48.14, H 3.12; found: C 47.91, H 3.12.

[Pd$_2$(tppb)Cl$_4$] (18): [Pd(CH$_3$CN)$_2$Cl$_2$] (72.6 mg, 0.28 mmol) was added, under nitrogen, to a solution of tppb (114.1 mg, 0.14 mmol) in dry CH_3CN (15 mL) and dry CH_2Cl_2 (15 mL). The yellow solution was stirred at room temperature in the dark overnight. The solvent was evaporated under vacuum and complex **18** (130 mg, 0.11 mmol, 80%) was purified by crystallization from ethyl ether. ^{1}H NMR (400 MHz, [D$_6$]DMSO): δ= 7.52 (d, ^3J=6.4 Hz, 16H; PPhH_o), 7.62 (t, ^3J=6.9 Hz, 8H; PPhH_p), 7.76 (m, 16H; PPhH_m), 8.02 ppm (brs, 2H; ArH); MALDI-TOF MS: *m/z* (%): calcd for $C_{54}H_{42}Cl_4P_4Pd_2$ (1169.4 amu) [M−Cl]$^+$: 1134.0; found: 1134 (70); calcd [M+K]$^+$: 1208.5; found: 1208 (20); elemental analysis calcd (%) for $C_{54}H_{42}Cl_4P_4Pd_2$: C 55.41, H 3.59; found: C 55.11, H 3.65.

[Pt$_2$(tppb)(CF$_3$SO$_3$)$_4$] (19): $AgCF_3SO_3$ (36 mg, 0.14 mmol) was added, under nitrogen, to a solution of compound **17** (48 mg, 0.035 mmol) in dry CH_3CN (10 mL) and dry CH_2Cl_2 (10 mL). The solution was stirred at 35 °C in the dark overnight; the white precipitate of AgCl formed was removed by filtration and the white solution was evaporated under reduced pressure. Complex **19** (33 mg, 0.018 mmol, 52%) was crystallized from ethyl ether. ^{1}H NMR (400 MHz, CD_3CN): δ=7.55 (m, 16H; PPhH_o), 7.59–7.72 (m, 24H; PPhH_p+PPhH_m), 8.10 ppm (brs, 2H; ArH); ESI-MS: *m/z* (%): calcd for $C_{58}H_{42}F_{12}O_{12}P_4Pt_2S_4$ (1801.2 amu) [M−CF$_3$SO$_3$]$^+$: 1652.2; found: 1652 (30); calcd [M−2CF$_3$SO$_3$]$^{2+}$: 751.6; found: 752 (100); calcd [M−3CF$_3$SO$_3$]$^{3+}$: 451.4; found: 452 (100).

[Pd$_2$(tppb)(CF$_3$SO$_3$)$_4$] (20): $AgCF_3SO_3$ (37 mg, 0.14 mmol) was added, under nitrogen, to a solution of compound **18** (42 mg, 0.036 mmol) in dry CH_3CN (10 mL) and dry CH_2Cl_2 (10 mL). The solution was stirred at room temperature in the dark overnight; the white precipitate of AgCl formed was removed by filtration and the yellow solution was evaporated under reduced pressure. The product was crystallized from ethyl ether to give complex **20** (36 mg, 0.022 mmol, 62%). ^{1}H NMR (400 MHz, CD_3NO_3): δ=7.60 (m, 16H; PPhH_o), 7.74–7.81 (m, 24H; PPhH_p+ PPhH_m), 8.32 ppm (brs, 2H; ArH); ESI-MS: *m/z* (%): calcd for $C_{58}H_{42}F_{12}O_{12}P_4Pd_2S_4$ (1623.9 amu) [M−CF$_3$SO$_3$]$^+$: 1474.9; found: 1475

(20); calcd $[M-2CF_3SO_3]^{2+}$: 662.9; found: 663 (20); calcd $[M-3CF_3SO_3]^{3+}$: 392.2; found: 392 (100).

General procedure for the self-assembly of dinuclear tetratopic cavitand complexes (21, 22): Dinuclear tetratopic cavitand complexes **21** and **22** were assembled by mixing cavitand **3** with complex **19**, and cavitand **6** with complex **20**, respectively, in a 4:1 molar ratio at room temperature in a $CHCl_3/CH_3NO_2/CH_3CN$ 7:2:1 mixture. After stirring for 15 min, the desired complexes **21** and **22** were obtained in quantitative yields after removal of the solvent under vacuum.

Data for 21: (M = Pt): ^{1}H NMR (400 MHz, $CDCl_3$): $\delta = 1.04$ (m, 48H; CH_3), 2.21 (m, 32H; CH_2-CH_3), 4.29 (m, 12H; ArCH_{in}), 4.47–4.57 (m, 16H; CHAr$_2$), 5.17 (s, 4H; CHPy), 5.63 (m, 12H; CH_{out}), 6.42 (s, 8H; ArH), 6.43 (s, 8H; ArH), 7.09 (s, 8H; ArH), 7.13 (s, 8H; ArH), 7.41–7.54 [m, 32H; PPhH_o + PPhH_p + PyH_m], 8.12 (brs, 2H; ArH), 8.93 ppm (m, (XX′ part of a AA′XX′ system), 8H; PyH_o); ESI-MS: *m/z* (%): calcd for $C_{238}H_{214}F_{12}N_4O_{44}P_4Pt_2S_4$ (4704.8 amu) $[M-2CF_3SO_3]^{2+}$: 2203.3; found: 2204 (10); calcd $[M-3CF_3SO_3]^{3+}$: 1419.2; found: 1419 (100).

Data for 22: (M = Pd): ^{1}H NMR (400 MHz, $CDCl_3$): $\delta = 1.06$ (m, 48H; CH_3), 2.21 (m, 32H; CH_2-CH_3), 4.26 (m, 12H; CH_{in}), 4.54 (m, 12H; CHAr$_2$), 4.65 (t, $^3J = 8.0$ Hz, 4H; CHAr$_2$), 5.29 (s, 4H; CHPhPy), 5.61 (m, 12H; CH_{out}), 6.42 (s, 8H; ArH), 6.51 (s, 8H; ArH), 7.12 (s, 8H; ArH), 7.17 (s, 8H; ArH), 7.38–7.68 (m, 48H; PPhH_o + PPhH_p + PyH_m + PyPhH_o + PyPhH_m), 8.17 (brs, 2H; ArH), 8.75 ppm (brs, 8H; *Py*H_o); ESI-MS: *m/z* (%): calcd for $C_{262}H_{230}F_{12}N_4O_{44}P_4Pd_2S_4$ (4831.8 amu) $[M-2CF_3SO_3]^{2+}$: 2266.8; found: 2266 (30); calcd [*M*−2CF_3SO_3–1 cavitand]$^{2+}$: 1865.8; found: 1865 (100).

Crystal structures: Crystals of compounds **9**, **10**, **11**, and *trans*-**12**, suitable for X-ray analysis, were obtained by slow diffusion of absolute ethanol into solutions of the compounds in CH_2Cl_2. Data collection was performed at the X-ray diffraction beamline facility (monochromatic wavelength $\lambda = 1.0000$ Å) of Elettra Synchrotron, Trieste (Italy), with a Mar CCD detector and by means of the rotating-crystal method. The crystals were soaked with an aqueous solution of PEG 1500 (50%, w/v) prior to mounting in loops and flash-cooling in a stream of nitrogen gas at 100 K. The diffraction data was indexed and integrated using MOSFLM[24] and scaled with SCALECCP4. The structures were solved by using the Patterson method (SHELXS)[25] and Fourier analyses, and refined by the full-matrix least-squares method based on F^2 (SHELXL-97).[26] The electron density maps showed one crystallographic-independent supramolecular complex in each structure, some dichloromethane and ethanol molecules of the crystallization solvent, and some water molecules coming from the cryoprotectant solution. In particular, the asymmetric units contained in **9**: 2 triflate counterions, 4.5 ethanol molecules, and 5 water molecules; in **10**: 1 dichloromethane molecule, 2 ethanol molecules, and 2 water molecules; in **11**: 2.5 dichloromethane molecules, 1 ethanol molecule, and 1.5 water molecules; in *trans*-**12**: 3.5 ethanol molecules and 2 water molecules. In the final refinement, all non-hydrogen atoms (except those of disordered solvent molecules) were treated anisotropically, and the hydrogen atoms were included at calculated positions with isotropic *U* factors = 1.2 U_{eq} of the carbon atom to which they were bonded. For **10** and **11**, the anisotropic thermal factors were restrained to an approximate isotropic behavior by using the card ISOR_* 0.5, because of the low observable/parameter ratios of these structures. Geometrical restraints were introduced for a few disordered solvent molecules. Crystal and refinement data are reported in Table 1.

A preliminary diffraction dataset from a crystal of the ditopic complex *trans*-**11**-bis, obtained from the $[Pt(dmso)_2Cl_2]$ route, was collected in-house (Bruker rotating anode generator and Kappa CCD2000) at room temperature by using monochromatic wavelength $\lambda = 1.5140$ Å. Crystals were monoclinic, $P2_1/n$, with unit cell parameters $a = 10.85(4)$, $b = 15.13(5)$, $c = 39.93(9)$ Å, $\beta = 95.24(8)°$; $V = 6345(8)$ Å^3; $Z = 2$; $\rho_{calcd} = 1.399$ g cm^{-3}. Even if this dataset was of poor quality and the refinement not completely satisfactory ($R1 = 0.231$, GOF = 1.533), analysis clearly confirmed that the structure of the *trans*-**11**-bis (Figure 6) was very similar to that of *trans*-**11**. The *trans* ditopic complexes were positioned on the crystallographic inversion centers located on the Pd ions with the chlorine ligands disordered over two positions.

CCDC-252894, -252895, -252896, and -252897 contain the supplementary crystallographic data for this paper. These data can be obtained free of charge from the Cambridge Crystallographic Data Centre via www.ccdc.cam.ac.uk/data_request/cif.

Table 1. Crystal data and structure refinement for **9**, *trans*-**10**, *trans*-**11**, and *trans*-**12**.

Compound	**9**	*trans*-**10**	*trans*-**11**	*trans*-**12**
formula	$(C_{129}H_{119}N_2O_{16}P_2Pt)$ 2(CF_3O_3S) 4.5(C_2H_6O)5(H_2O)	$(C_{53}H_{47}Cl_2N_2O_8Pt)$ 2(C_2H_6O) 2-(H_2O) 1(CH_2Cl_2)	$(C_{102}H_{94}Cl_2N_2O_{16}Pt)$ 2.5(CH_2Cl_2) 1(C_2H_6O) 1.5(H_2O)	$(C_{53}H_{43}Cl_2NO_9PtS)$ 3.5-(C_2H_6O) 2(H_2O)
M_r	2800.78	1316.99	2155.19	1336.23
crystal system, space group	triclinic, $P\bar{1}$	triclinic, $P\bar{1}$	monoclinic, $P2_1/c$	monoclinic, $P2_1/n$
a [Å]	12.32	10.85	10.86	10.85
b [Å]	23.17	15.34	28.10	15.13
c [Å]	25.85	19.40	35.18	38.93
α [°]	72.6	108.0	90	90
β [°]	83.6	92.4	91.1	96.9
γ [°]	87.1	106.4	90	90
V [Å^3]	6995	2916	10737	6345
Z	2	2	4	4
ρ_{calcd} [g cm^{-3}]	1.330	1.500	1.333	1.399
μ [mm^{-1}]	1.62	4.124	2.49	3.669
$F(000)$	2902	1334	4424	2728
$\lambda/2\sin\theta_{max}$ [Å]	0.95	1.00	0.985	1
unique reflns	15292	3809	10355	6610
reflns [$I > 2\sigma(I)$]	12057	3415	7862	5782
parameters	1676	656	1212	701
restraints	38	396	786	6
GOF	1.247	1.057	1.533	1.049
R [$I > 2\sigma(I)$]	$R1 = 0.111$	$R1 = 0.070$	$R1 = 0.134$	$R1 = 0.081$
	$wR2 = 0.285$	$wR2 = 0.191$	$wR2 = 0.349$	$wR2 = 0.231$
R (all data)	$R1 = 0.127$	$R1 = 0.075$	$R1 = 0.150$	$R1 = 0.087$
	$wR2 = 0.307$	$wR2 = 0.197$	$wR2 = 0.370$	$wR2 = 0.240$

Acknowledgements

This work was supported by MURST (FIRB-Nano-organization of Materials with Magnetic and Optical Properties and COFIN-2003-Single Molecule Addressing on Surfaces). A special thanks goes to Prof. E. Alessio (University of Trieste) for helpful suggestions. The instrumental facilities at the Centro Interfacoltà di Misure G. Casnati of the University of Parma were used. We are grateful for the help of the beam-line scientists at the Elettra synchrotron facility.

[1] M. M. Conn, J. Rebek, Jr., *Chem. Rev.* **1997**, *97*, 1647–1668.
[2] L. Pirondini, E. Dalcanale, *Encyclopedia of Nanoscience and Nanotechnology*, Marcel Dekker, New York, **2004**, pp. 3415–3430.
[3] For selected examples of ditopic calixarene receptors see: a) K. Araki, K. Hisaichi, T. Kanai, S. Shinkai, *Chem. Lett.* **1995**, 569–570; b) J. Wang, C. D. Gutsche, *J. Am. Chem. Soc.* **1998**, *120*, 12226–12231; c) T. Haino, M. Yanase, F. Fukazawa, *Angew. Chem.* **1998**, *110*, 1044–1046; *Angew. Chem. Int. Ed.* **1998**, *37*, 997–998; d) A. Arduini, A. Pochini, A. Secchi, *Eur. J. Org. Chem.* **2000**, 2325–2334; e) J. Wang, S. G. Bodige, W. H. Watson, C. D. Gutsche, *J. Org. Chem.* **2000**, *65*, 8260–8263.
[4] a) D. J. Cram, L. M. Tunstad, C. B. Knobler, *J. Org. Chem.* **1992**, *57*, 528–535; b) I. Higler, P. Timmerman, W. Verboom, D. N. Reinhoudt, *J. Org. Chem.* **1996**, *61*, 5920–5931; c) I. Higler, W. Verboom, F. C. J. M. van Veggel, F. de Jong, D. N. Reinhoudt, *Liebigs Ann./Recl.* **1997**, 1577–1586; d) R. G. Chapman, J. C. Sherman, *J. Am. Chem. Soc.* **1998**, *120*, 9818–9826; e) F. C. Tucci, A. R. Renslo, D. M. Rudkevich, J. Rebek, Jr., *Angew. Chem.* **2000**, *112*, 1118–1121; *Angew. Chem. Int. Ed.* **2000**, *39*, 1076–1079; f) U. Lucking, F. C. Tucci, D. M. Rudkevich, J. Rebek, Jr., *J. Am. Chem. Soc.* **2000**, *122*, 8880–8889; g) S. D. Starnes, D. M. Rudkevich, and J. Rebek, Jr., *J. Am. Chem. Soc.* **2001**, *123*, 4659–4669; h) J. L. Irwin, M. S. Sherburn, *Org. Lett.* **2001**, *3*, 225–227; i) E. S. Barrett, J. L. Irwin, P. Turner, M. S. Sherburn, *Org. Lett.* **2002**, *4*, 1455–1458; j) A. Lützen, O. Hass, T. Bruhn, *Tetrahedron Lett.* **2002**, *43*, 1807–1811; k) L. M. Tunstad, J. E. Nunez, S.-W. Kang, C. E. Godinez, 219th ACS National Meeting San Francisco, CA, Abstr., p. 111.
[5] S. Leininger, B. Olenyuk, P. J. Stang, *Chem. Rev.* **2000**, *100*, 853–908.
[6] H. Xi, C. L. D. Gibb, E. D. Stevens, B. C. Gibb, *Chem. Commun.* **1998**, 1743–1744.
[7] J. O. Green, J.-H. Baird, B. C. Gibb, *Org. Lett.* **2000**, *2*, 3845–3848.
[8] a) L. Pirondini, F. Bertolini, B. Cantatori, F. Ugozzoli, C. Massera, E. Dalcanale, *Proc. Natl. Acad. Sci. USA* **2002**, *99*, 4911–4915; b) R. Pinalli, V. Cristini, V. Sottili, S. Geremia, M. Campagnolo, A. Caneschi, E. Dalcanale, *J. Am. Chem. Soc.* **2004**, *126*, 6516–6517.
[9] Ligand exchange experiments with coordination cages formed by pyridyl-bridged cavitands and Pt–dppp showed, upon heating to 50°C, fast formation/dissociation of this type of complex (see ref. [8a]).
[10] The stereochemical purity of *cis*-$[Pt(CH_3CN)_2Cl_2]$ was checked by both FTIR and ^1H NMR spectroscopy. See: F. P. Fanizzi, F. P. Intini, L. Maresca, G. Natile, *J. Chem. Soc. Dalton Trans.* **1990**, 199–202.
[11] P.-C. Kong, F. D. Rochon, *Can. J. Chem.* **1978**, *56*, 441–445.
[12] H. Yuan, L. Thomas, L. K. Woo, *Inorg. Chem.* **1996**, *35*, 2808–2817.
[13] The assignment was performed on the basis of literature data of [Pt(dmso)(py)Cl_2] complexes: G. Annibale, M. Bonivento, L. Cattalini, M. L. Tobe, *J. Chem. Soc. Dalton Trans.* **1992**, 3433–3438.
[14] C. Tessier, F. D. Rochon, *Inorg. Chim. Acta* **1999**, *295*, 25–38.
[15] a) P. H. Dinolfo, J. T. Hupp, *Chem. Mater.* **2001**, *13*, 3113–3125; b) S. J. Lee, W. Lin, *J. Am. Chem. Soc.* **2002**, *124*, 4554–4555.
[16] a) D. Vitali, F. Calderazzo, *Gazz. Chim. Ital.* **1972**, *102*, 587–596; b) P. J. Giordano, M. S. Wrighton, *J. Am. Chem. Soc.* **1979**, *101*, 2888–2897.
[17] a) A. D. McMorran, P. J. Steel, *Angew. Chem.* **1998**, *110*, 3495–3497; *Angew. Chem. Int. Ed.* **1998**, *37*, 3295–3297; b) L. Pirondini, D. Bonifazi, E. Menozzi, E. Wegelius, K. Rissanen, C. Massera, E. Dalcanale, *Eur. J. Org. Chem.* **2001**, 2311–2320; c) L. Pirondini, A. G. Stendardo, S. Geremia, M. Campagnolo, P. Samorì, J. P. Rabe, R. Fokkens, E. Dalcanale, *Angew. Chem.* **2003**, *115*, 1422–1425; *Angew. Chem. Int. Ed.* **2003**, *42*, 1384–1387.
[18] H. C. E. McFarlane, W. McFarlane, *Polyhedron* **1988**, *7*, 1875–1879.
[19] P. J. Stang, D. H. Cao, S. Saito, A. M. Arif, *J. Am. Chem. Soc.* **1995**, *117*, 6273–6283.
[20] R. Pinalli, M. Suman, E. Dalcanale, *Eur. J. Org. Chem.* **2004**, 451–462.
[21] a) S. Levi, P. Guatteri, F. C. J. M. van Veggel, G. J. Vancso, E. Dalcanale, D. N. Reinhoudt, *Angew. Chem.* **2001**, *113*, 1945–1948; *Angew. Chem. Int. Ed.* **2001**, *40*, 1892–1896; b) E. Menozzi, R. Pinalli, E. A. Speets, B. J. Ravoo, E. Dalcanale, D. N. Reinhoudt, *Chem. Eur. J.* **2004**, *10*, 2199–2206.
[22] L. Tunstad, J. A. Tucker, E. Dalcanale, J. Weiser, J. A. Bryant, J. C. Sherman, R. C. Helgeson, C. B. Knobler, D. J. Cram, *J. Org. Chem.* **1989**, *54*, 1305–1312.
[23] J. H. Price, A. N. Williamson, R. F. Schramm, B. B. Wayland, *Inorg. Chem.* **1972**, *11*, 1280–1284.
[24] Collaborative Computational Project, Number 4, *Acta Crystallogr. Sect. D* **1994**, *50*, 760–763.
[25] G. M. Sheldrick, *Acta Crystallogr. Sect. A* **1990**, *46*, 467–473.
[26] G. M. Sheldrick, SHELXL-97, University of Göttingen, Göttingen (Germany), **1997**.

Received: October 19, 2004
Published online: March 17, 2005